2003

A high-resolution surface vector wind product for coastal oceans: Blending satellite scatterometer measurements with regional mesoscale atmospheric model simulations

Chao, Yi; Li, Zhijin; Kindle, John C.; Paduan, Jeffrey D.; Chavez, Francisco P.

American Geophysical Union

Chao, Y., Z. Li, J. C. Kindle, J. D. Paduan, and F. P. Chavez, A high-resolution surface vector wind product for coastal oceans: Blending satellite scatterometer measurements with regional mesoscale atmospheric model simulations, Geophys. Res.Lett., 30(1), 1013, doi:10.1029/2002GL015729, 2003.

https://hdl.handle.net/10945/46663

GEOPHYSICAL RESEARCH LETTERS, VOL. 30, NO. 1, 1013, doi:10.1029/2002GL015729, 2003

A high-resolution surface vector wind product for coastal oceans: Blending satellite scatterometer measurements with regional mesoscale atmospheric model simulations

Yi Chao
Jet Propulsion Laboratory, California Institute of Technology, Pasadena, California, USA

Zhijin Li
Raytheon ITSS, Pasadena, California, USA

John C. Kindle
Naval Research Laboratory, Stennis Space Center, Mississippi, USA

Jeffrey D. Paduan
Naval Postgraduate School, Monterey, California, USA

Francisco P. Chavez
Monterey Bay Aquarium Research Institute, Moss Landing, California, USA

Received 22 June 2002; revised 23 September 2002; accepted 25 September 2002; published 8 January 2003.

[1] A 2-dimensional variational method is used to blend the satellite scatterometer measured (QuikSCAT) and regional mesoscale atmospheric model simulated (COAMPS) surface vector winds for coastal central California. The approach is distinct from existing methods in that it considers errors from both measurements and models. When compared with independent in situ observations, the blended wind product shows consistently higher correlation and smaller RMS errors than QuikSCAT or COAMPS winds. The proposed algorithm can be implemented over any part of the world ocean. It should be a valuable tool for describing small-scale atmospheric processes in coastal zones and for forcing high-resolution coastal ocean models. *INDEX TERMS:* 4275 Oceanography: General: Remote sensing and electromagnetic processes (0689); 3332 Meteorology and Atmospheric Dynamics: Mesospheric dynamics; 3307 Meteorology and Atmospheric Dynamics: Boundary layer processes; 3337 Meteorology and Atmospheric Dynamics: Numerical modeling and data assimilation; 4279 Oceanography: General: Upwelling and convergences. **Citation:** Chao, Y., Z. Li, J. C. Kindle, J. D. Paduan, and F. P. Chavez, A high-resolution surface vector wind product for coastal oceans: Blending satellite scatterometer measurements with regional mesoscale atmospheric model simulations, *Geophys. Res. Lett.*, *30*(1), 1013, doi:10.1029/2002GL015729, 2003.

1. Introduction

[2] Atmospheric circulation over the ocean is modified close to continents by coastal topography creating small-scale variability in the wind field. In addition, coastal winds are difficult to measure from space due to land contamination. Given that the coastal winds are highly variable, difficult to measure remotely, and important in driving ocean variability, we investigated the possibility of blending coastal winds from high resolution atmospheric models and from satellite scatterometers. The initial demonstration for this technique was carried out in coastal central California.

[3] The coastal ocean of central California is dominated by coastal upwelling. Upwelling is, to first order, a dynamical response to local wind forcing. Alongshore upwelling favorable wind drives Ekman transport that moves surface water offshore. The transport divergence at the coastline draws deeper water towards the surface. The spatial gradients in wind or wind curl can also drive the divergence. The resultant "Ekman pumping" is a fundamental forcing agent for coastal circulation and variability. The characteristic signature of upwelling is a cool band of sea surface temperature along the coast, typically tens of kilometers wide. This cool band is separated from warmer offshore waters by a series of fronts, plumes, and eddies. These features can extend more than 100 km offshore.

[4] Ocean models have been typically forced with real-time or archived products from atmospheric operational centers. These products were generated by either a global model or a limited-area forecast model if available for the region of interest. Satellite scatterometry (e.g., the SeaWinds scatterometer on the QuikSCAT satellite) provides an alternative to model-generated fields by producing surface wind measurements with global coverage at relatively high spatial and temporal resolutions. QuikSCAT is capable of providing wind measurements for operational users in near real-time (less than 3 hours delay for 90% of the observations). However, its application in the coastal ocean is rather limited because the standard QuikSCAT data product has a spatial resolution on the order of 25 km, while coastal features can have smaller spatial scales. Further land contamination hampers satellite scatterometer data in coastal zones. Since the QuikSCAT footprint is an ellipse approximately 25-km in azimuth by 37-km in the look (or range) direction and wind retrieval requires fore- and aft-look observations, land (or sea ice) can contami-

0094-8276/03/2002GL015729$05.00

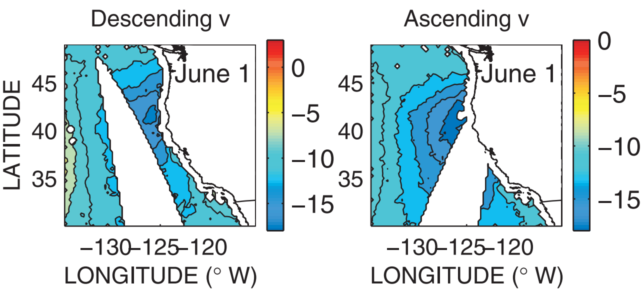

Figure 1. The Level 3 QuikSCAT surface vector winds (in m s^{-1}) binned on a 25 $\times$ 25 km grid on June 1, 2000, for both the ascending and decending passes. The white area in the ocean represents the data gap.

nate data within 25–37 km from the coast (Figure 1). In addition to the intrinsic difficulties in measuring the wind near the coast, the complex spatial and temporal sampling of the scatterometer further introduces noise to the gridded wind maps. Even though this noise does not appear in the interpolated wind fields, it becomes problematic when computing wind gradients (e.g., wind curl and divergence), particularly at the edges of the satellite swath (Figure 2a).

[5] To overcome these difficulties, the present study attempts to combine the satellite-measured surface vector winds with winds obtained by a regional mesoscale atmospheric model. Blending satellite-derived winds with atmospheric model winds has been proposed since the advent of satellite wind observations [e.g., *Atlas et al.*, 1996; *Tang and Liu*, 1996; *Chin et al.*, 1998; *Pegion et al.*, 2000]. However, the previous investigations all focused on global applications and didn't consider the unique characteristics of the coastal zones. The objective of the present study is to generate a high-resolution surface vector wind product specifically for coastal applications. This letter describes our proposed blending algorithm. Central California coast was selected for the initial demonstration because of the availability of both long-term in situ wind observations and a 9-km regional COAMPS^{tm} (Coupled Ocean/Atmosphere Mesoscale Prediction System) model [*Hodur*, 1997].

2. A 2D-Var Blending Algorithm

[6] Our proposed algorithm is based on the 2-dimensional variational (2D-Var) method. The method of 2D-Var can be mathematically described by minimizing the total cost function as defined by:

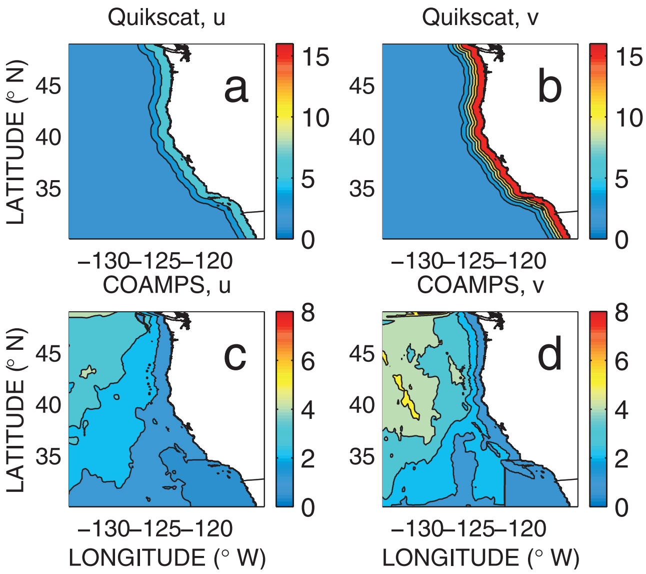

Figure 3. Maps of error variance (in m^2 s^{-2}) of the zonal and meridional wind components for QuikSCAT and COAMPS^{tm}.

$$J_{total} = J_q + J_c + J_{curl} + J_{div}, \quad (1)$$

where the cost functions for QuikSCAT (J_q) and COAMPS^{tm} (J_c) are defined by:

$$J_q = 0.5(U_q - H_qU)^T Q_u^{-2}(U_q - H_qU) + 0.5(V_q - H_qV)^T Q_v^{-2}(V_q - H_qV), \quad (2)$$

$$J_c = 0.5(U_c - U)^T C_u^{-2}(U_c - U) + 0.5(V_c - V)^T C_v^{-2}(V_c - V). \quad (3)$$

Here U and V are the blended zonal and meridional wind components (on the COAMPS^{tm} grid). q and c stand for QuikSCAT and COAMPS^{tm}, and Q and C are the error covariance matrices for QuikSCAT and COAMPS^{tm}, respectively. The dimension of these error covariance matrices corresponds to the total number of COAMPS^{tm}

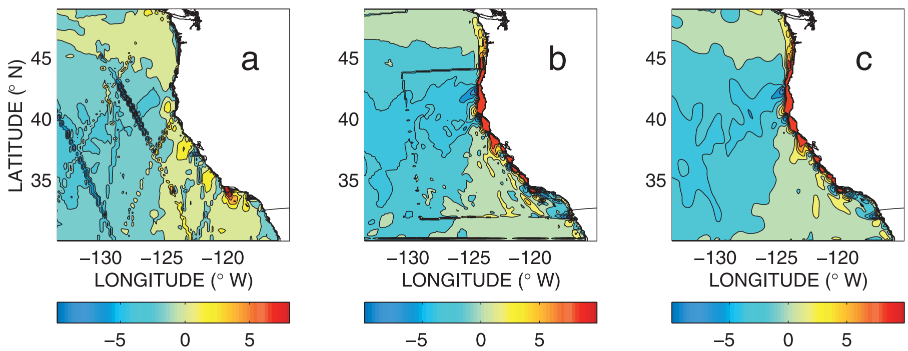

Figure 2. Daily maps (June 1, 2000) of the wind curl (in 10^{-6} s^{-1}) as derived from the QuikSCAT data (a), simulated by the COAMPS^{tm} model (b), and the blended product (c).

Table 1. Correlation and RMS Error (m s^{-1}) Comparing Daily QuikSCAT, COAMPS^{tm}, and the Blended QuikSCAT/COAMPS^{tm} Winds Against in Situ Mooring Observations at Three Mooring Locations

	M1				M2				M3			
	Correlation		RMS		Correlation		RMS		Correlation		RMS	
	U	V	U	V	U	V	U	V	U	V	U	V
QuikSCAT	0.69	0.56	2.1	4.0	0.65	0.86	2.4	2.4	0.78	0.89	1.8	2.2
COAMPS^{tm}	0.80	0.89	1.9	1.4	0.86	0.93	1.6	1.7	0.86	0.91	1.8	2.0
Blended	0.87	0.91	1.8	1.3	0.86	0.95	1.7	1.5	0.90	0.96	1.5	1.3

The M1 (122.03°W, 36.75°N), M2 (122.39°W, 36.75°N), and M3 (122.96°W, 36.57°N) moorings are located 20-km, 55-km, and 100-km offshore, respectively. The M1 and M2 data cover the period of 1 August 1999 to 30 September 2000, while the M3 data cover the period of 1 August 1999 to 6 March 2000.

grid points. $\boldsymbol{H_q}$ is a spatial interpolation operator transforming the QuikSCAT data onto the COAMPS^{tm} grid. $()^T$ represents the transpose of a matrix.

[7] An important feature of the proposed method is the additional terms in the total cost function introduced to control the spurious gradient in the blended wind fields. Because of the complex spatial and temporal sampling patterns of QuikSCAT, a simple interpolation in space and time often introduces spurious wind gradient along the edges of satellite swaths (Figure 2a). The COAMPS^{tm} model, on the other hand, may exhibit spurious values near the boundaries of the model nests for situations in which a blending scheme is used to provide fields for a domain larger than the finest model (Figure 2b). Thus, an optimal combination of the satellite-based QuikSCAT and model-simulated COAMPS^{tm} should suppress these spurious gradients of wind that are apparent in the wind divergence and wind curl fields. Based on these considerations, we introduce two additional terms in the total cost function:

$$\boldsymbol{J_{curl}} = 0.5\boldsymbol{W_c}^{-2}|\nabla(\xi - \xi_{clim})|^2, \tag{4}$$

$$\boldsymbol{J_{div}} = 0.5\boldsymbol{W_d}^{-2}|\nabla(\psi - \psi_{clim})|^2, \tag{5}$$

where ξ and ψ represent the wind curl and divergence, and $\boldsymbol{W_c}$ and $\boldsymbol{W_d}$ are weighting coefficients for wind curl and divergence, respectively. The subscript *clim* represents the background climatological field.

3. Error Estimation and Minimization Procedure

[8] In this study, we consider only the diagonal form of $\boldsymbol{Q_u}$, $\boldsymbol{Q_v}$, $\boldsymbol{C_u}$, $\boldsymbol{C_v}$, and their diagonal elements are simply the

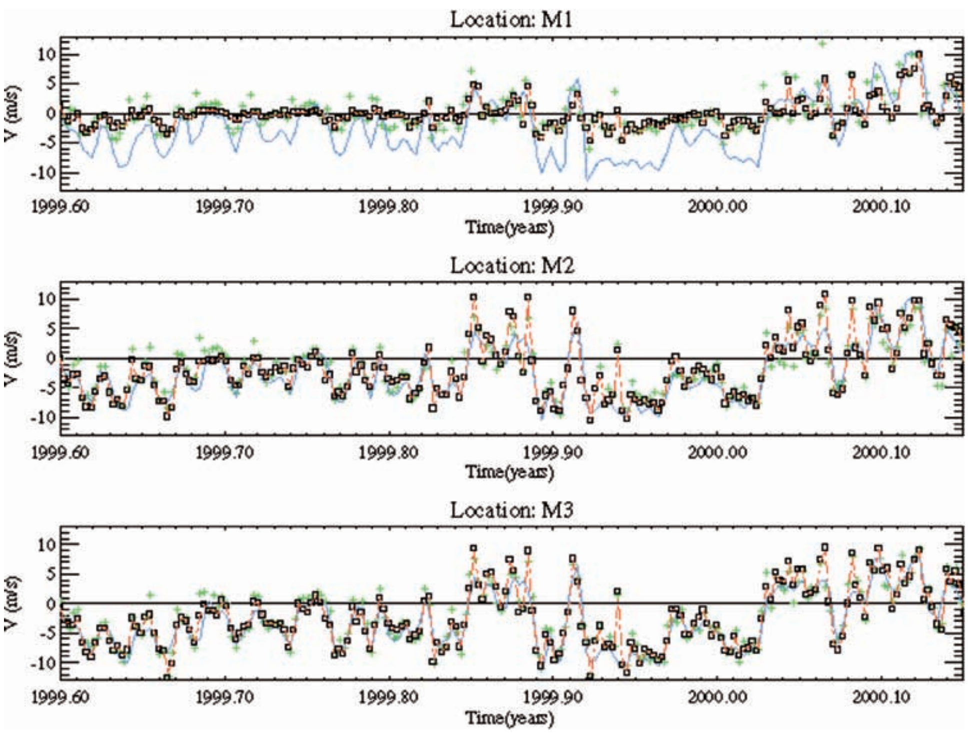

Figure 4. Time series of daily meridional wind component (in m s^{-1}) at three mooring locations, M1 (122.03°W, 36.75°N), M2 (122.39°W, 36.75°N), and M3 (122.96°W, 36.57°N). The time covers the period from 1 August 1999 to 6 March 2000. The mooring data are cross symbols in green, QuikSCAT in blue solid lines, COAMPS^{tm} in black square, and the blended analyses are dotted-dash lines in red.

error variances estimated below. An optimal estimation has to take into account errors from both measurements and models. However, the available wind observations are too sparse to directly compute the error variance, which has to be estimated indirectly. In this study, we assume that errors of QuikSCAT and COAMPS^{tm} are independent. This assumption is justified because the QuikSCAT data are not assimilated into the current version of COAMPS^{tm} used here. This assumption leads to an important relationship:

$$\langle (U_c - U_q)^2 \rangle = dQ_u + dC_u, \tag{6}$$

$$\langle (V_c - V_q)^2 \rangle = dQ_v + dC_v, \tag{7}$$

where $\langle\rangle$ represents the time mean. dQ and dC represent the error variances and correspond to the diagonal element of the Q and C matrices. Both Q and C are estimated by comparing QuikSCAT with independent mooring observations off the central California coast. In the open ocean, dQ_u and dQ_v are assumed uniform. In the coastal ocean, dQ_u and dQ_v are assumed as a function of offshore distance (d), i.e.,

$$dQ_u = a_u + b_u\, exp(-d/d_u)^2, \tag{8}$$

$$dQ_v = a_v + b_v\, exp(-d/d_v)^2. \tag{9}$$

Parameters (a_u, b_u, d_u, a_v, b_v, d_v) are determined by an empirical fit between the QuikSCAT data and mooring observations. Once dQ_u and dQ_v are estimated, dC_u and dC_v can be simply derived from equations (6) and (7). A salient feature of the COAMPS^{tm} error is its increase offshore (Figures 3c and 3d), exactly opposite to the QuikSCAT error (Figures 3a and 3b). This error structure justifies our proposed approach of using the QuikSCAT data to improve the COAMPS simulation, particularly away from the coast.

[9] In this study, daily winds from both QuikSCAT and COAMPS^{tm} are used. To start the twice daily QuikSCAT Level 3 data with a resolution of 25 $\times$ 25 km are first interpolated onto the COAMPS^{tm} grid with no spatial and temporal smoothing. The daily QuikSCAT data are obtained by averaging the ascending and decending satellite passes, which are approximately 12 hours apart. The hourly COAMPS^{tm} data with a resolution of 9-km are averaged into daily means. The QuikSCAT and COAMPS^{tm} winds are then used to generate the blended product by minimizing the total cost function (J_{total}) using the limited-memory quasi-Newton minimization method [*Noceadal and Liu*, 1989].

4. Summary of Results and Concluding Remarks

[10] Comparisons of the three wind products (QuikSCAT, COAMPS^{tm}, and the blended wind) against independent in situ observations are provided in Table 1 and Figure 4. QuikSCAT and mooring observations agree well at offshore mooring locations, i.e., M2 (55-km away from coastline) and M3 (100-km away from coastline). The error of QuikSCAT winds increases dramatically at the M1 mooring location, which is approximately 20-km from the coastline. This is due to the lack of valid QuikSCAT wind measurements within two 25 $\times$ 25 km grid cells from the coastline and the inability of QuikSCAT wind measurements to resolve the significant diurnal (i.e., sea breeze) fluctuations observed at the M1 location.

[11] The blending algorithm puts more (less) weight on QuikSCAT in the offshore (near-shore) region, and puts more (less) weight on COAMPS^{tm} in the near-shore (offshore) region, according to their error structures. The resulting optimal combination of QuikSCAT and COAMPS^{tm} consistently shows an increase in correlations and a reduction of RMS errors in both coastal and offshore locations. At offshore locations (e.g., M3), the RMS error of QuikSCAT is comparable to that of COAMPS^{tm}. The blending algorithm is able to reduce the RMS error for both QuikSCAT and COAMPS^{tm} at offshore locations. These optimal features distinguish our approach from those designed for global gridded wind products.

[12] Another important feature of the blended wind product is the pronounced positive (or cyclonic) wind curl along the California coast. The blended wind product (Figure 2c) is significantly better in describing this fundamental feature near the continental boundaries than QuikSCAT (Figure 2a) and COAMPS (Figure 2b). In summary, the proposed blending algorithm should be a valuable tool for coastal environments that are difficult to observe with the current generation of scatterometer satellites.

[13] **Acknowledgments.** The research described in this paper was carried out, in part, at the Jet Propulsion Laboratory, California Institute of Technology, under contract with the National Aeronautics and Space Administration (NASA). Support from National Oceanographic Partnership Program (NOPP) is acknowledged. The participation of JCK was also funded through the Naval Research Laboratory (NRL) 6.1 CoBALT ARI and the Dynamics of Coupled Models project under program element 61153N sponsored by the Office of Naval Research. We thank Dudley Chelton, Michael Freilich, and Jim McWilliams for many stimulating discussions on the topics related to surface winds. We also acknowledge Rich Hodur, Sergio deRada, Reiko Michisaki, and Fred Bahr for providing various wind data sets. The QuikSCAT Level 3 gridded data set is obtained from the anonymous FTP site (http://podaac.jpl.nasa.gov: pub/ocean_wind/quikscat/L3).

References

Atlas, R., R. Hoffman, S. Bloom, J. Jusem, and J. Ardizzone, A multi-year global surface wind velocity data set using SSM/I wind observations, *Bull. Amer. Meteoro. Soc.*, *77*, 869–882, 1996.

Chin, T. M., R. F. Milliff, and W. G. Large, Basin-scale, high-wavenumber sea surface wind fields from a multiresolution analysis of scatterometer data, *J. Atmos. Oceanic Tech.*, *15*, 741–763, 1998.

Hodur, R. M., The Naval Research Laboratory's Coupled Ocean/Atmosphere Mesoscale Prediction System (COAMPS), *Mon. Wea. Rev.*, *125*, 1414–1430, 1997.

Nocedal, J., and D. C. Liu, On the Limited Memory Method for Large Scale Optimization, *Mathematical Programming B*, *45*(3), 503–528, 1989.

Pegion, P. J., M. A. Bourassa, D. M. Legler, and J. J. O'Brien, Objective derived daily "winds" from satellite scatterometer data, *Mon. Wea. Rev.*, *128*, 3150–3168, 2000.

Tang, W., and W. T. Liu, Objective interpolation of scatterometer winds, JPL Tech. Publication 96-19, 16 pp., 1996.

Y. Chao, Jet Propulsion Laboratory, 4800 Oak Grove Drive, MS 300-323 Pasadena, CA 91109, USA. (Yi.Chao@jpl.nasa.gov)

F. P. Chavez, Monterey Bay Aquarium Research Institute, Moss Landing, CA 95039, USA. (chfr@mbari.org)

J. C. Kindle, Naval Research Laboratory, Stennis Space Center, MS 39529, USA. (kindle@nrlssc.navy.mil)

Z. Li, Raytheon ITSS, 299 N. Euclid Av. Suite 500, Pasadena, CA 91101, USA. (zhijin@pacific.jpl.nasa.gov)

J. D. Paduan, Naval Postgraduate School, Monterey, CA 93943, USA. (paduan@nps.navy.mil)